

# Multi-Vehicle Flocking: Scalability of Cooperative Control Algorithms using Pairwise Potentials

Yao-Li Chuang<sup>1,2</sup>, Yuan R. Huang<sup>3</sup>, Maria R. D’Orsogna<sup>1</sup>, Andrea L. Bertozzi<sup>1</sup>

**Abstract**—In this paper, we study cooperative control algorithms using pairwise interactions, for the purpose of controlling flocks of unmanned vehicles. An important issue is the role the potential plays in the stability and possible collapse of the group as agent number increases. We model a set of interacting Dubins vehicles with fixed turning angle and speed. We perform simulations for a large number of agents and we show experimental realizations of the model on a testbed with a small number of vehicles. In both cases, critical thresholds exist between coherent, stable, and scalable flocking and dispersed or collapsing motion of the group.

## I. INTRODUCTION

### A. Motivation

Social aggregation is a remarkable aspect of animal behavior. Large numbers of individual agents interacting with each other are able to self-organize into complex yet coordinated patterns such as insect swarms, fish schools and bird flocks [1]. These systems have recently become of great interest for the mathematical [2], physical [3], [4] and biological sciences [5] with promising applications for the development and control of autonomous, multi-vehicular ensembles [6], [7]. One main goal of this nascent field of research is to program interactions among individuals so that desired collective behaviors arise. Spatial patterns, however, can be dramatically affected even by small parameter changes, not only in the interactions, but also in constituent number or speed [8]. In this paper, we formulate criteria, valid for *general* pairwise interactions, to ensure local group cohesion of a first order model. When interactions are controlled by a Morse potential, we investigate stability and scalability through numerical simulations and practical testbed applications, demonstrating the existence of thresholds and cutoffs for different regimes of aggregation.

### B. Related work and outline

Swarming vehicular systems are often modeled as point particles in which members may interact with one another through pairwise interactions; these are perhaps the most important features in determining what, and if, patterns will form. A class of attractive and repulsive pairwise potentials has been studied in Ref. [4] where self-propelled particles were shown to self-organize into coherent two dimensional patterns. The existence of cohesive and bound swarms has

also been reported in Refs. [9], [10], [11]. More recently, for aggregates of similarly interacting, self-propelled agents, stabilization or collapse with respect to particle number has been predicted [8]. In other studies, virtual leaders [6] and structural potential functions [12] have been introduced to direct and stabilize vehicles into desired formations or to avoid obstacles. Furthermore, the robustness of various algorithms in the presence of noise, communication delays and other non-idealities, have been tested on several testbeds, both for single and multi-vehicular systems [13], [14]. Activities such as spatial dispersion, gradient navigation, and cluster formation have also been reported [15] as well as single-vehicle path following, stationary obstacle avoidance, and cooperative searching [16].

In section II we present a general theory applicable to first order dynamical systems subject to pairwise potential interactions and we find local conditions for flock cohesion. In section III we adapt our model to a group of Dubins vehicles [17], [18] with specific attractive and repulsive interactions. We discuss stability and scalability of the system for certain parameter ranges, and we also investigate the effects of virtual leaders. Finally, in section IV, results from numerical simulations and experimental realizations of the model for small vehicle numbers are shown.

## II. THEORY

We consider a general potential flow for a particle at position  $\vec{r}_i$ , at distance  $r_i = |\vec{r}_i|$  from the origin, subject to dissipation  $\gamma$  and to pairwise interactions  $U$ :

$$\dot{\vec{r}}_i = -\gamma \vec{\nabla}_i \sum_{j \neq i} U(r_{i,j}). \quad (1)$$

Here  $r_{i,j} \equiv |\vec{r}_i - \vec{r}_j|$  denotes the distance between agents  $i, j$ . For simplicity in the remainder of this paper we will set  $\gamma = 1$ . The potential  $U$  has an attractive and repulsive part denoted by  $U_a, U_r$ , respectively. Then,  $U' = U'_a - U'_r$ , with  $U'_a, U'_r \geq 0$ . The center of mass  $\vec{x} = \sum_{i=1}^N \vec{r}_i$  is stationary for any interaction potential that depends solely on the distance between agents. Without loss of generality we let  $\vec{x} = 0$ . The first order, ‘kinematic’ model of Eqn. 1 has been intensely studied in the literature from both biological [2] and control points of view [9]. In Ref. [9], Gazi and Passino define a *free agent* to be one whose distance to all other members of the swarm is greater than the repulsive length scale of the potential. Free agents interacting through an ad-hoc potential, in which the repulsive part is bounded and the attractive part has a parabolic, spring-like shape centered about zero, are

<sup>1</sup>Dept. of Mathematics, University of California Los Angeles, Los Angeles, CA 90095 {chuang, dorsogna, bertozzi}@math.ucla.edu

<sup>2</sup>Dept. of Physics, Duke University, Durham, NC 27708

<sup>3</sup>Dept. of Electrical Engineering, University of California Los Angeles, Los Angeles, CA 90095 yuanh@seas.ucla.edu

proven to converge to an absorbing ball around the center of mass. The convergence time is finite. A crucial point in the proof is the parabolic shape of the potential, and its strong, attractive, yet unphysical, nature at infinite distances. One important feature of this result is that all agents collapse inside the absorbing region, regardless of constituent number  $N$  and initial condition. The radius of the absorbing ball is in fact independent of  $N$  so that as  $N \rightarrow \infty$ , the density of the final resting state diverges as well. The dynamics of Eqn. 1 is a gradient flow for the total energy  $U_{tot} = \sum_{j \neq i} U(r_{i,j})$ . We are concerned with finding general conditions on  $U$  for which this result can be proved *locally*, that is if all agents start inside a fixed set. Related to this system, is one that involves second order dynamics:

$$\dot{\vec{r}}_i = \vec{v}_i, \quad \dot{\vec{v}}_i = f(v_i) \vec{v}_i - \vec{\nabla}_i \sum_{j \neq i} U(r_{i,j}). \quad (2)$$

This Newtonian description has been used in several models [4], [8], [12], [20]. Self propulsion and drag of an individual are introduced through  $f$ , and the potential  $U$  is as above. The system is conservative if  $f = 0, \forall v$  and often  $f$  is chosen so that there exists a special value  $v^*$  for which  $f(v^*) = 0$ . In fact, as pumping and dissipation occur through  $f$ , it is reasonable to expect that the steady state configurations of Eqn. 2 are minimizers of the energy  $U_{tot}$  and zeroes of  $f$ . In Ref. [8], Eqn. 2 is studied in the context of how potential parameter choices affect swarming patterns.

Drawing on analogies with statistical ensembles [19], an important indicator of the expected morphology is found to be the *H-stability* of the interaction potential  $U$ . A system is said to be H-stable if the energy per particle is bounded from below as the number of particles goes to infinity. Non H-stable potentials are called ‘catastrophic’ as they typically result in systems that collapse as the number of particles increases. While such systems are of lesser interest in classical statistical physics, they largely dominate the literature on swarming as they more often give rise to cohesive motion of a group, as in the case studied by Gazi and Passino. Their global cohesion result is due to the unphysical parabolic potential at infinity which gives each agent unbounded velocity at large distances. In this paper, we prove that the results of Ref. [9] for first order systems can be extended to a much broader class of potentials, provided we consider local stability in which agents are initially confined to a bounded region of space. In this paper we also make analogies between first and second order models of the type shown in Eqns. 1 and 2 and study how their stable equilibria scale with particle number. We make the following definition:

*Definition 1 : Diffused state.* A flock is in a *diffused state* if  $r_{i,j} > \delta \forall i \neq j$ , where  $\delta$  is the repulsive range such that  $U'(r) > 0$  for all  $r > \delta$ .

Note that in order to be in a diffused state, the potential must yield only attraction outside of a certain radius. The following Lemma shows that, regardless of the specific form of the potential, a diffused state always shrinks.

*Lemma 1 : Weak maximum principle.* Define the flock radius as  $R \equiv \sup_i r_i$ . For a flock in the diffused state,  $\dot{R} \leq 0$ .

*Proof :* Let  $R = r_i$  and define  $\hat{r}_{i,j} \equiv \vec{r}_{i,j}/r_{i,j}$ . Then:

$$\frac{\dot{r}_i^2}{2} = \vec{r}_i \cdot \dot{\vec{r}}_i = -\vec{r}_i \cdot \sum_{j \neq i} \hat{r}_{i,j} U'(r_{i,j}) \quad (3)$$

$$= \sum_{j \neq i} \frac{(\vec{r}_i \cdot \vec{r}_j - r_i^2)}{r_{i,j}} U'(r_{i,j}) \leq 0 \quad (4)$$

since  $r_i^2 \geq \vec{r}_i \cdot \vec{r}_j$  and  $U' > 0$  in the diffused state. Thus  $r_i^2$ , and  $r_i$ , are decreasing functions and  $\dot{R} \leq 0$ .  $\square$

A corollary to the above Lemma 1 is that the swarm size decreases even if only the outermost agents are in a diffused state. This is due to the fact that the proof only uses an estimate for the farthest agents of the swarm. We now prove a local stability limit for general interactions  $U$  and find conditions for particles initially constrained to a local region of radius  $R$ , to evolve into a more compact ball of radius  $R^* < R$ . The proof uses a Lyapunov function discussed in [9], [10].

*Theorem 1 :* Consider  $N$  particles located at  $\vec{r}_i$  with  $r_i \leq R \forall i, 1 \leq i \leq N$ . If a finite constant value  $K > 0$  exists such that  $\max_{\{0 \leq r \leq 2R\}} |Kr - U'(r)| < KR$ , then asymptotically  $r_i \leq R^*$ , with  $R^* < R$ .

*Proof :* We choose the Lyapunov function  $V_i = r_i^2/2$ . Its time derivative obeys the following

$$\dot{V}_i = -\vec{r}_i \cdot \vec{\nabla}_i \sum_{j \neq i} U(r_{i,j}) \quad (5)$$

$$= -\vec{r}_i \cdot \sum_{j \neq i} \hat{r}_{i,j} U'(r_{i,j}) \quad (6)$$

$$\leq -KNr_i^2 + r_i(N-1)\eta, \quad (7)$$

where  $\eta \equiv \max_{\{r_{i,j} \leq 2R\}} |Kr - U'(r)|$ . In going from Eqn. 6 to Eqn. 7 we have added and subtracted  $Kr_{i,j}$  where  $K > 0$  is an arbitrary constant. We also used the fact that  $\vec{r}_i \cdot \sum_{j \neq i} \vec{r}_{i,j} = Nr_i^2$ . Also note that  $r_{i,j} \leq 2R$  since by assumption  $r_i \leq R$ . Asymptotically then:

$$r_i \leq \frac{N-1}{N} \frac{\eta}{K} \leq \frac{\eta}{K} \equiv R^*, \quad (8)$$

and we require  $\eta < KR$  for this bound to be more stringent than the initial radius  $R$ .  $\square$

*Corollary 1:* If Theorem 1 holds for all  $R' < R$  then as  $t \rightarrow \infty$  the system will collapse with all particles converging at  $R_f = 0$ .

*Proof :* This follows from the fact that for  $r_i \geq \eta/K$ , the Lyapunov function  $\dot{V} \leq -Kr_i^2 = -2KV_i$ . The limit  $R^*$  is thus reached in a time:

$$t_{max} = \max_i \left[ \frac{1}{2K} \ln \left( \frac{\eta^2}{2K^2 V_i(0)} \right) \right], \quad (9)$$

where  $V_i(0)$  is the Lyapunov function at time  $t = 0$ . After  $t_{max}$  is reached, Theorem 1 can be applied again, and the iteration process can be repeated until the limit  $R_f = 0$  is reached. Theorem 1, applied to the parabolic potential of Ref. [9] is the global convergence theorem there shown. Our control algorithm adopts a generalized Morse potential that decays at infinite distances, as would be expected for systems of vehicles with a limited communication range:

$$U(r_{i,j}) = -C_a e^{-r_{i,j}/\ell_a} + C_r e^{-r_{i,j}/\ell_r}. \quad (10)$$

Here,  $C_a, C_r$  represent the strength of the attractive and repulsive potentials, and  $\ell_a, \ell_r$  their length scales, respectively. Define  $\ell \equiv \ell_r/\ell_a$ ,  $C \equiv C_r/C_a$ . A sufficient condition for Theorem 1 is

$$\left( \frac{C_a}{\ell_a} e^{-\frac{2R}{\ell_a}} - \frac{C_r}{\ell_r} \right) < 2KR < 2 \left( \frac{C_a}{\ell_a} e^{-\frac{2R}{\ell_a}} - \frac{C_r}{\ell_r} \right), \quad (11)$$

which can be satisfied only if  $\ell > C$  so that  $R$  can be chosen as  $2R < \ell_a \ln(\ell/C)$ . Also note that Corollary 1 holds here, since the latter condition holds for all  $R' < R$ . The above condition is a sufficient but not necessary one, and other combinations of  $\ell, C$  could give rise to acceptable  $R, K$  values without resulting in a state where all agents collapse to a point. It is interesting to compare these results with the stability phase diagram of Ref. [8] for the same potential in the second order model of Eqn. 2. The region  $\ell > C$  with  $\ell < 1$  is classified as catastrophic in Ref. [8], with particles converging towards their center of mass and becoming denser as  $N \rightarrow \infty$ . This is consistent with the results proven here that  $N$  particles initially in a ball of radius  $R$  get ‘squeezed’ into a tighter one. On the other hand, the region  $\ell > C$ , with  $\ell > 1$  is classified as stable in Ref. [8], with no possible squeezing effects in the long time limit. The apparent discrepancy can be understood as follows. In the region  $\ell > C, \ell > 1$ , the pairwise potential has a positive, local minimum for  $r_{i,j} = 0$  and a barrier at  $r_{i,j} = r_{max} > \ell_a \ln(\ell/C)$ , before decaying to zero as  $r_{i,j} \rightarrow \infty$ . The first order system (1) is purely dissipative and there are no fluctuations in the total energy, which can only decrease in time. For second order systems of the type described in Eqn. 2 however, even if the local energy minimum is reached, with all particles simultaneously at  $r_{i,j} = 0$ , fluctuations due to exchange with the environment as imposed by  $f$ , can eventually drive the system away, towards the dispersed, global energy minimum at  $r_{i,j} \rightarrow \infty$ . For other, specific choices of the potential parameters, numeric estimates can determine whether  $R, K$  values exist that satisfy Theorem 1.

### III. TESTBED ADAPTATION

The models described in Eqns. 1 and 2 cannot be directly applied to a platform of autonomous vehicles due to mechanical constraints. The platform of real vehicles we use is described in Ref. [14]. The vehicles consist of Dubins micro-cars with fixed speed and fixed left and right turning radii. The first constraint implies our dynamical system must be described as first order. The only independent variable denoting agent

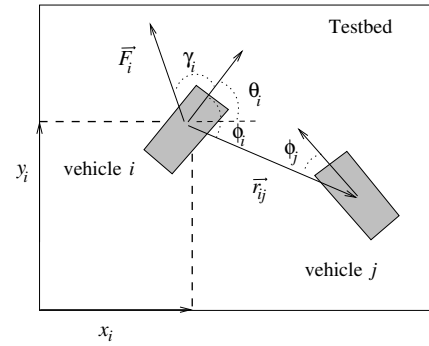


Fig. 1. Definition of variables for vehicle  $i$ : The heading is denoted by  $\theta_i$ , the angle between its direction of motion and the  $x$  axis of the testbed.  $\vec{F}_i$  is the interaction force it experiences due to all other vehicles. This direction defines an angle  $\gamma_i$  with the heading direction. Vehicle  $i$  is at a distance  $\vec{r}_{i,j}$  from vehicle  $j$  and the angles  $\phi_i$  and  $\phi_j$  here shown are used in the collision avoidance scheme described in the text. The origin of the reference coordinate system is fixed at the left-lower corner of the testbed. All vehicular angles,  $\gamma_i, \theta_i, \phi_i$ , are defined in  $[\pi, -\pi)$ .

$i$  is its heading angle with respect to a fixed orientation we define as  $\theta_i$ . The Dubins vehicles interact with each other by means of the Morse potential of Eqn. 10 with variable parameters  $C_a, C_r, \ell_a, \ell_r$ . Due to the fixed turning radii, the interactions cannot directly control  $\theta_i$  and an appropriate control algorithm must be devised. For each vehicle then, we measure the angle  $\gamma_i$  between vehicle heading and the total force  $\vec{F}_i$  it experiences, as given by the right hand side of Eqn. 1 and as shown in Fig. 1. Vehicle  $i$  then changes direction only if  $|\gamma_i| > \Gamma$ , where  $\Gamma$  is an angular threshold  $0 \leq \Gamma \leq \pi$ . The equations of motion are as follows:

$$\dot{x}_i = \alpha \cos \theta_i \quad \dot{y}_i = \alpha \sin \theta_i, \quad (12)$$

$$\dot{\theta}_i = \begin{cases} \frac{\alpha}{R_L} & \text{if } \gamma_i > \Gamma \quad (\text{left turn}), \\ -\frac{\alpha}{R_R} & \text{if } \gamma_i < -\Gamma \quad (\text{right turn}), \\ \frac{\alpha}{R_S} & \text{otherwise.} \end{cases} \quad (13)$$

Here,  $\alpha$  is the speed of the vehicle, and  $R_L, R_R$  are the left and right turning radii, respectively.  $R_S$  is the deviation radius. In the ideal case  $R_L = R_R$  and  $R_S = \infty$ , so that vehicle direction is unaffected for  $|\gamma_i| < \Gamma$ . Because of alignment asymmetries in general  $R_L \neq R_R$  and  $R_S$  is a large but finite number. Vehicular motion proceeds along the direction specified by the heading parameter  $\theta_i$  until the turning commands  $\dot{\theta}_i$  are given.

A crucial point is that the interaction potential in Eqn. 10 is soft-core and does not prevent vehicles from colliding. In fact, even hard-core potentials cannot avoid collisions due to communication delays, errors in position information, and the finite turning radius of the vehicles. The repulsive range may be increased to initiate turning at larger inter-vehicle distances. This however, would significantly affect pattern formation and the emergence of cooperative aggregates would be unlikely. Instead, we add an additional collision avoidance algorithm to address short range interactions. We use a ‘wait and go’ scheme for vehicles closer than a

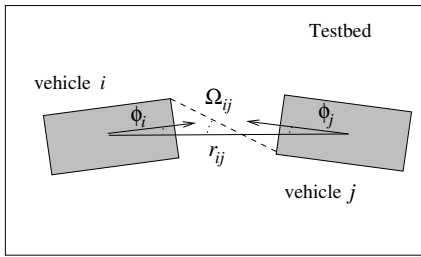


Fig. 2. Collision avoidance failure: The angles  $\phi_i$  and  $\phi_j$  are too small and vehicles  $i$  and  $j$  collide even if one of them should pause. An additional algorithm is required to steer the vehicles away from each other and is described in the text. It relies on the angle  $\Omega_{i,j}$  here depicted.

cutoff distance  $r_c$ . For vehicles  $i, j$  at distance  $\vec{r}_{i,j}$  such that  $r_{i,j} < r_c$ , we define the angles  $\phi_i, \phi_j$  between their main axis and  $\vec{r}_{i,j}$ , as shown in Fig. 1. If  $\phi_i < \phi_j$  vehicle  $i$  will pause while vehicle  $j$  veers away, until  $r_{i,j} > r_c$ . The cutoff distance  $r_c$  in the control algorithm acts as an effective hard-core potential. If  $\phi_i = \phi_j$  any one of the vehicles (in our simulations the one with a higher labeling index) will pause and let the other proceed. When  $\phi_i, \phi_j \simeq 0$  the 'wait and go' scheme cannot avoid collision as shown in Fig. 2, and an alternate algorithm is invoked. For vehicles  $i$  and  $j$  we define the angle  $\Omega_{i,j}$  between  $\vec{r}_{i,j}$  and the segment joining their opposite front edges measured from  $\max\{\phi_i, \phi_j\}$  as shown in Fig. 2. If  $\max\{\phi_i, \phi_j\} < \Omega$ , where  $\Omega$  is an angular threshold  $0 \leq \Omega \leq \pi/2$ , then the vehicle closer to the center of the testbed is veered towards the center and the other in the opposite direction.

#### IV. EXPERIMENTAL RESULTS

In this section we study the behavior and performance scaling of a set of Dubins vehicles controlled by the first order laws based on the model in the previous section. We consider both testbed implementation and numerical simulations for small and large numbers of vehicles, respectively. The computer model is validated against the testbed in the case of a few vehicles. It is also possible to incorporate the presence of many virtual vehicles in practical testbed applications and study the effects of larger vehicle numbers on the actual ones.

##### A. Testbed Simulations

The testbed has three working vehicles. A virtual leader moves around an ellipse with semimajor axis approximately 15 times the vehicle length. There is some variability in vehicle speed. To address this issue, the position of the leader is checked against the distance to the closest vehicle. If the distance becomes larger than a certain threshold  $d_t$ , the leader will pause; otherwise, it will move at its intrinsic speed, We select our parameters as follows:  $\ell_r = 5.7$  cm,  $\ell_a = 95.2$  cm,  $C_a = 10^4$  erg and  $C_r = 6 \cdot 10^3$  erg. so that  $C = 1.67$  and  $\ell = 0.06$ . Note that these parameters correspond to a potential in the 'catastrophic regime' of Ref. [8]. For potential parameters in the H-stable regime we have not been able to realize stable configurations of vehicular aggregation due, in part, to the constant speed of the vehicles. The leader interacts

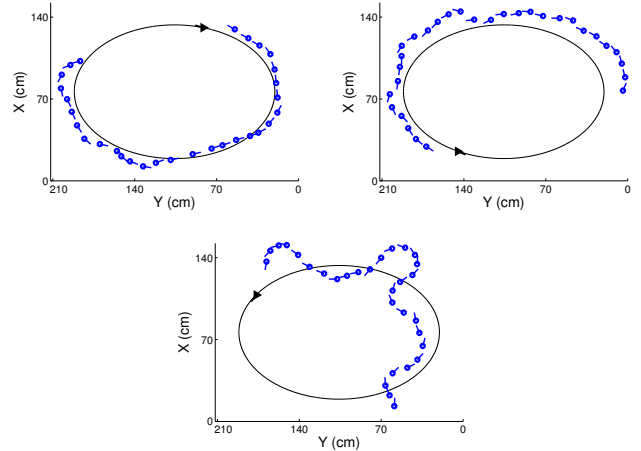


Fig. 3. Vehicular motion: These panels show fragments of the vehicle's trajectory when it tries to follow a virtual leader along an elliptical path. The vehicle is unstable when  $d_t$  is decreased below  $r_{eq} = 20.2$  cm. Top left:  $d_t = 20.5$  cm; Top right:  $d_t = 20.2$  cm; Bottom:  $d_t = 20.0$  cm.

with the vehicles according to the same Morse potential used for vehicle-vehicle interaction. When leading more than one vehicle, the leader's contribution to the potential is increased 1.1 times and 2.1 times the vehicular potential for the two-vehicle and the three-vehicle experiments, respectively.

1) *One vehicle follows a leader:* The parameters mentioned above provide short-range repulsion and long-range attraction resulting in an equilibrium separation. Fig. 3 shows results for  $d_t$  near the equilibrium  $r_{eq}$ , calculated to be  $r_{eq} = 20.2$  cm. Running tests with  $d_t = 20.5$  cm,  $d_t = 20.2$  cm, and  $d_t = 20.0$  cm, we note that leader-following becomes ineffective for  $d_t$  below  $r_{eq}$ .

2) *Two vehicles follow a leader:* The vehicles are found to alternate between a snake-like competing behavior as shown in Fig. 4-top and a stable gliding behavior as shown in Fig. 4-middle. The stable behavior emerges when one vehicle trails the other and they form a rather flat triangle with the leader that glides around the ellipse as shown in Fig. 4-bottom.

3) *Three vehicles follow a leader:* The vehicles still alternate between competing and gliding behaviors as in the two-vehicle case as shown in Fig. 5-top. When stable motion emerges, the vehicles and the leader form a stretched quadrilateral that glides around the ellipse as shown in Figs. 5-middle and bottom. We note that fragmentation can sometimes occur due to the stretched formation, as the attraction between the two slower vehicles overwhelms the long-range attraction from the leader.

To reduce such occurrences, we can enhance the leader attraction by increasing its weight. Also, both group cohesion and stabilization of the above examples can be realized by imposing rigid formations for the vehicle group as in Ref. [6]. Note, however, that in the absence of a rigid structure, even though the vehicles shift position with respect to each other, they are able to maintain a coherent group as they follow the leader around the track.

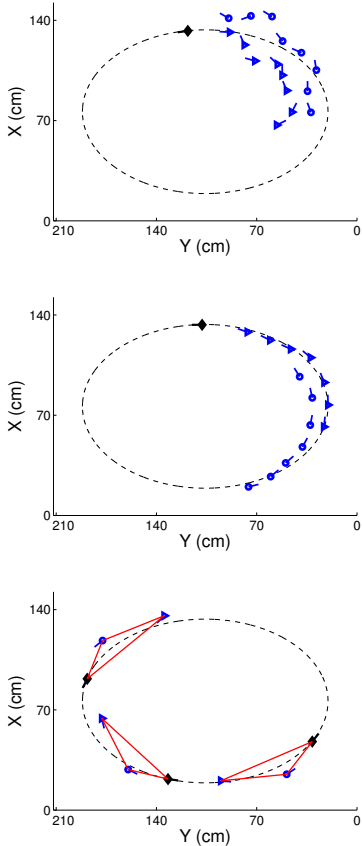


Fig. 4. Two vehicles try to follow a virtual leader along an elliptical path. Top: Two vehicles exhibit snake-like motion as they compete for the optimal spot behind the virtual leader; middle and bottom: The vehicles' motion becomes stable when one trails the other, and they form a flat triangle with the leader, which glides along the path.

### B. Computer Simulations

Computer simulations provide a powerful tool to study scalability and statistical issues for large numbers of vehicles. Fig. 6 shows two distinct formations observed in computer simulations of 100 vehicles. Aggregates similar to the vortex shown in the left-hand panel of Fig. 6 are seen for weak or non-existent leaders. For strong, effective leaders, vehicles align and follow, as shown in the right hand panel. For the second-order model of Eqn. 2 as specified in Ref. [8] it is shown that as the number of agents increase, collapse, stability or dispersion of the agents depend on the parameters of the potential. It is interesting to investigate how these results compare to the first-order model of Eqns. 12 and 13. In particular, in Ref. [8] it is shown that for a range of parameter values defined by  $C$  and  $\ell$  coherent behavior is expected. In Fig. 7 we show the steady state formation radius as a function of vehicle number in the catastrophic regime, where coherent structures are expected to collapse as the number of constituents increases. In the present model, the size of a catastrophic flock remains steady as vehicle number increases, consistent with an increasing vehicle density. On the other hand, for parameter values

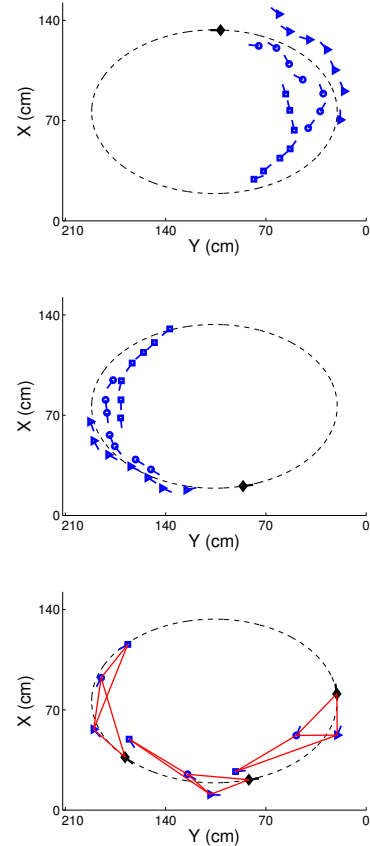


Fig. 5. Three vehicles try to follow a virtual leader along an elliptical path. Top: Vehicles exhibit snake-like motion when they level with each other; Middle: The formation becomes stable when one trails another. Bottom: The vehicles and the leader form a stretched quadrilateral that glides along the path.

in the H-stable regime, where aggregation is extensive in large number limit, the flock size expands with increasing vehicle number. Repulsion is more accentuated in the the H-stable regime: for parameters that are close to the stable-catastrophic threshold flocking is still possible, but as the parameters are chosen further and further away into the H-stable regime, cooperative flocks no longer occur and vehicle groups loose coherence. Fig. 8 shows that the critical  $\ell_r$ , beyond which the flock disintegrates is located deeper into the H-stable regime as the number of vehicles increases.

### V. CONCLUSIONS

We consider a well-known first order gradient flow model for robot interactions in a swarm. We prove new results on cohesion and collapse for a general class of potentials. In particular, we find conditions under which the system is guaranteed to converge inside a ball of fixed radius, provided it started from a ball of pre-defined larger radius. These radii are independent of number of agents and result in a state in which swarm density goes to infinity as vehicle number increases. Such scaling results are very important in designing large agent swarming algorithms. We adapt the model to a system of Dubins vehicles and consider

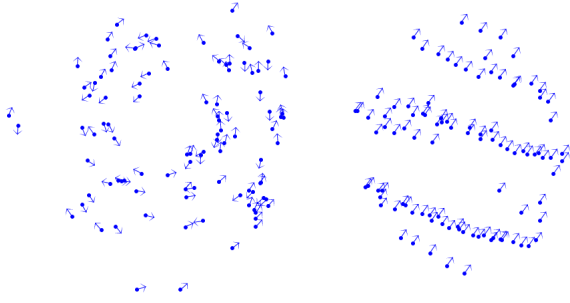


Fig. 6. Vehicular formations in the presence of a leader: The formation to the left occurs when the vehicles fall out of the leader's path and self-aggregate into a vortex-like formation. The formation to the right occurs when the vehicles successfully follow the leader.

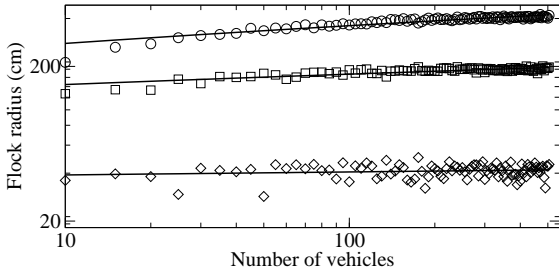


Fig. 7. Scaling in the H-stable and catastrophic regimes. The potential parameters are set at  $\ell_a = 95.2$  cm,  $C_a = 10^4$  erg and  $C_r = 6 \cdot 10^3$  erg. With these parameter choices, H-stability is guaranteed for  $\ell_r > 73.5$  cm. In the top curve  $\ell_r = 76.2$  cm, in the middle one,  $\ell_r = 69.0$  cm, just below the transition threshold. The bottom curve, for which  $\ell_r = 35.7$  cm, falls deeply into the catastrophic regime. Straight lines are power law fits with powers  $10^{-1}$ ,  $10^{-2}$  for the top and middle set. Within fitting errors, the catastrophic curve defines a constant flocking radius.

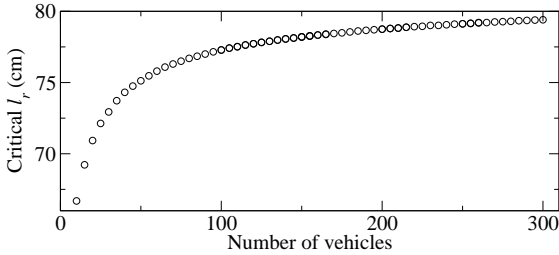


Fig. 8. Critical  $\ell_r$  versus vehicle number. The data points indicate the  $\ell_r$  threshold beyond which the cooperative flock disintegrates.  $C_r, C_a, \ell_a$  are the same as in Fig. 7

both testbed and numerical simulations for the swarm. We include a virtual leader which allows for continued motion of the swarm in a confined geometry. For small numbers of agents, the testbed verifies some simple facts about stability of the algorithm under certain parameters of the virtual leader potential. For large numbers of agents we show in computer simulations how the size of the swarm scales as the agent number increases. In our model, as the number of agents grows, the swarm is able to maintain its cohesion using potentials with parameters that would lead to instability at smaller numbers.

## VI. ACKNOWLEDGMENTS

This research was supported by ONR grant N000140610059 and ARO grant W911NF-05-1-0112.

## REFERENCES

- [1] S. Camazine, J. L. Deneubourg, N. R. Franks, J. Sneyd, G. Theraulaz, and E. Bonabeau, *Self organization in biological systems*, Princeton University Press, Princeton, NJ, 2003.
- [2] A. Mogilner, L. Edelstein-Keshet, L. Bent and A. Spiros, "Mutual interactions, potentials, and individual distance in a social aggregation", *J. Math. Biol.* Vol. 47, pp. 353-389, 2003.
- [3] T. Vicsek, A. Czirok, E.B. Jacob, I. Cohen, and O. Schochet, "Novel type of phase transitions in a system of self-driven particles", *Phys. Rev. Lett.* Vol. 75, pp. 1226-1229, 1995.
- [4] H. Levine, W. J. Rappel, and I. Cohen "Self-organization in systems of self-propelled particles", *Phys. Rev. E*, Vol. 63, pp. 017101, 2000.
- [5] I. D. Couzin, J. Krause, R. James, G. D. Ruxton, and N. R. Franks, "Collective memory and spatial sorting in animal groups", *J. Theor. Biol.*, Vol. 218, pp. 1-11, 2002.
- [6] N. E. Leonard and E. Fiorelli, "Virtual leaders, artificial potentials, and coordinated control of groups", in *Proc. Conf. Decision Contr.*, Orlando, FL, pp. 2968-2973, 2001.
- [7] A. Jadbabaie, J. Lin, and A. S. Morse, "Coordination of groups of mobile autonomous agents using nearest neighbor rules", *IEEE Trans. Autom. Contr.*, Vol. 48, pp. 988-1001, 2003.
- [8] M. R. D'Orsogna, Y. L. Chuang, A. L. Bertozzi and L. Chayes, "Self-propelled particles with soft-core interactions: patterns, stability, and collapse", *Phys. Rev. Lett.*, vol. 96, 2006, to appear.
- [9] V. Gazi and K. Passino, "Stability analysis of swarms", in *IEEE Trans. Autom. Contr.* Vol. 48, pp. 692-697, 2003.
- [10] V. Gazi and K. Passino, "A class of attractions/repulsion functions for stable swarm aggregations", in *Proc. Conf. Decision Contr.*, Las Vegas, NV, pp. 2842-2847, 2002.
- [11] V. Gazi and K. Passino, "Stability analysis of social foraging swarms: combined effects of attractant/repellent profiles", in *Prof. Conf. Decision Contr.*, Las Vegas, NV, pp. 2848-2853, 2002.
- [12] R. Olfati-Saber and R. M. Murray, "Distributed cooperative control of multiple vehicle formations using structural potential functions", in *IFAC World Congress*, Barcelona, Spain, 2002. [http://thayer.dartmouth.edu/~olfati/papers/ifac02\\_ros\\_rmm.pdf](http://thayer.dartmouth.edu/~olfati/papers/ifac02_ros_rmm.pdf)
- [13] L. Cremean, W. Dunbar, D. V. Gogh, J. Kickey, E. Klavins, J. Meltzer, R. M. Murray, "The Caltech Multi-Vehicle Wireless Testbed", in *Proc. Conf. Decision Contr.*, Las Vegas, NV, pp.86-88, 2002; Z. Jin, S. Waydo, E. B. Wildanger, M. Lammers, H. Scholze, P. Foley, D. Held, and R. M. Murray, "MVWT-II: The second generation Caltech Multi-Vehicle Wireless Testbed", in *Proc. American Contr. Conf.*, Boston, MA, pp. 5321-5326, 2004.
- [14] C. H. Hsieh, Y. L. Chuang, Y. Huang, K. K. Leung, A. L. Bertozzi, and E. Frazzoli, "An economical micro-car testbed for validation of cooperative control strategies", in *Proc. American Contr. Conf.*, Minneapolis, MN, 2006, to appear.
- [15] J. McLurkin, *MIT Computer Science and Artificial Intelligence Laboratory*, <http://people.csail.mit.edu/jamesm/>
- [16] B. Q. Nguyen, Y. L. Chuang, D. Tung, C. Hsieh, Z. Jin, L. Shi, D. Marthaler, A. L. Bertozzi, and R. M. Murray, "Virtual attractive-repulsive potentials for cooperative control of second order dynamic vehicles on the Caltech MVWT", in *Proc. American Contr. Conf.*, Portland, OR, pp. 1084-1089, 2005.
- [17] L. E. Dubins, "On curves of minimal length with a constraint on average curvature and with prescribed initial and terminal positions and tangents", *Am. J. Math.*, Vol. 79, pp. 497-516, 1957.
- [18] A. M. Shkel and V. J. Lumelsky, "Classification of the Dubins set", *Robotics and Autonomous Systems*, Vol. 34, pp. 179-202, 2001.
- [19] D. Ruelle, *Statistical Mechanics, rigorous results*, W. A. Benjamin Inc, New York, NY, 1969.
- [20] R. Olfati-Saber, "Flocking for multi-agent dynamic systems: algorithms and theory", *IEEE Trans. on Autom. Contr.*, Vol. 51, 2006, to appear.